

Numerical solutions to two-body problems in classical electrodynamics: Head-on collisions with retarded fields and radiation reaction. I. Repulsive case*

J. Huschilt and W. E. Baylis

Physics Department, University of Windsor, Windsor, Ontario, Canada N9B 3P4

(Received 18 August 1975)

Classical trajectories of two particles with like charges have been computed numerically for head-on collisions. The trajectories are physical solutions of the Lorentz-Dirac equation with retarded fields. To eliminate runaway solutions, the third-order equation has been integrated numerically backward in time. Results are presented both for the static case (one particle is infinitely massive) and for two particles of equal mass. In the latter case, iterations are required in order to obtain self-consistent trajectories. Compared to results with the Lorentz equation, in which radiation reaction is ignored, maximum accelerations are markedly smaller, distances of closest approach are larger, and there is a small loss in particle energy rather than a large gain. No evidence was found for a lower bound on the distance of closest approach or for an upper bound on the radiated energy.

I. INTRODUCTION

The interaction of two charged particles is a basic problem of classical electrodynamics, and in the head-on collision of two like-charged particles it takes its simplest form. It is desirable to know whether reasonable solutions can be calculated in order to both test the classical theory and, we hope, gain insight into some related questions of quantum electrodynamics. It is surprising that the problem has resisted previous attempts at solution.

Past difficulties have arisen both from the need to use retarded potentials and from the practically pathological character of the third-order Lorentz-Dirac equation.

It was evidently the difficulty with retarded potentials that, until recently,¹ deterred adequate treatment of the head-on collision problem with even the relatively simple second-order Lorentz equation, in which self-radiation reaction is omitted. However, the difficulties are handled straightforwardly by storing trajectory information in arrays which can later be accessed to compute retarded quantities.

The pathological character of the Lorentz-Dirac equation has received considerable attention.² As Dirac first pointed out, the third-order equation is incomplete without a boundary condition on the acceleration $\ddot{x}(t)$.³ With the usual prescription (and the one we adopt here), namely $\ddot{x}(t \rightarrow \infty) \rightarrow 0$, one selects a physical trajectory from what is otherwise a continuum of unphysical solutions. Of course the prescribed condition does not depend on computational considerations. However, there is a strong asymmetry in the stability of the Lorentz-Dirac equation to backward and forward integration. In the usual forward numerical integration

of the third-order equation, the boundary condition at $t = +\infty$ is difficult to apply and runaway contributions to the solution grow extremely fast, roughly as $\exp(e^t)$. Even the physical solution itself has seemingly undesirable characteristics, such as noncausal preacceleration and an essentially unlimited self-energy source of radiative energy. Dissatisfaction with the Lorentz-Dirac equation has led some authors to suggest new equations of motion for charged particles.⁴ However, these generally have not proved entirely satisfactory.⁵

A way around the problem of runaway solutions is to integrate the third-order equation *backward* in time. The runaway contribution is then rapidly damped to zero (see below). Problems in which a single charged particle moves in finite fields of known space-time dependence are thus solved with relative ease, and indeed the existence of solutions for this case has been established.⁵ A few examples of motion in static fields of fixed (infinitely massive) point charges are given in Sec. II.

However, for the general interaction of two particles the fields depend on past trajectories and solutions using backward time integration require an iteration procedure for the particle paths. The question of whether physical solutions exist is in this case much more complex. A convergent iterative technique is presented in Sec. III and results are discussed in Sec. IV.

II. MOTION IN STATIC FIELDS

In the limit that one particle is much more massive than the other, the problem reduces to finding the motion of the lighter particle in the static field of the other. The solution is relatively simple; a single integration of the third-order Lorentz-Dirac equation, moving backward in time, is sufficient.

Energy is radiated only by the lighter particle and can be computed by integrating the relativistic Larmor power formula.⁷ By computing trajectories for this case and comparing radiated energies with losses in particle energies, we have a check of the adequacy both of the Lorentz-Dirac equation and of our integration methods.

The Lorentz-Dirac equation for a particle of charge e and renormalized mass m is³

$$ma^\mu = eF^{\mu\nu}u_\nu + \Gamma^\mu, \tag{1}$$

where $F^{\mu\nu}$ is the external retarded field, Γ^μ is the Abraham four-vector

$$\Gamma^\mu = \frac{2}{3}e^2(da^\mu/d\tau - a^\nu a_\nu u^\mu), \tag{2}$$

and $\tau, u^\mu \equiv dx^\mu/d\tau$, and $a^\mu \equiv d^2x^\mu/d\tau^2$ are, respectively, the proper time, the four-velocity, and the four-acceleration. Units with $c = 1$ have been used. We consider a particle of unit charge and mass ($e = m = 1$) colliding head-on with a massive second particle of the same charge. The magnetic field vanishes on the trajectory in this case so that Eq. (1) reduces to

$$\ddot{x} = \gamma^{-3}E + \frac{2}{3}\gamma(\dot{x}' + 3\dot{x}^2\dot{x}\gamma^2), \quad \gamma = (1 - \dot{x}^2)^{-1/2} \tag{3}$$

where dots here indicate time derivatives in the center-of-momentum frame. If the second particle is fixed at the origin, the electric field E is simply

$$E = x^{-2}. \tag{4}$$

If the third-order equation (3) is numerically integrated forward in time, an unphysical runaway solution can build up rapidly from unavoidable small round-off errors to terms of dominant size in about $1.5N$ time units, where N is the number of significant figures used in the computation. (A time unit is the time required for light to travel the classical charge radius and is about 10^{-23} sec for an electron.) The origin of the runaway solutions is readily seen by casting Eq. (3) into the form

$$\frac{d}{d\tau}(\gamma' e^{-3\tau/2}) = -\frac{3}{2}E e^{-3\tau/2}, \tag{5}$$

where $\gamma' = d\gamma/dx$. A small error ϵ resulting from the integration of the right-hand side over τ will give a runaway contribution to γ' which grows as $e^{3\tau/2}\epsilon$. Since $\gamma' = (\gamma^2 - 1)^{-1/2}d\gamma/d\tau$, γ itself will increase by $\cosh(e^{3\tau/2}\epsilon)$. However, if we integrate backward in time, errors ϵ will be damped as $e^{-3\tau/2}\epsilon$, and we can also ensure that the asymptotic condition ($a \rightarrow 0$ as $\tau \rightarrow \infty$) is satisfied. Furthermore, trajectories will not depend sensitively on the final acceleration (we chose the Lorentz value, $\ddot{x}_F = \gamma^{-3}E$).

Plass used backward integration to obtain a trajectory for a particle colliding at velocity $V_I \approx 0.1$ with the static field of a point charge.⁶ However, he did not compare radiated energy and mechanical energy lost.

We have extended the Plass results to final velocities $V_F \leq 0.96$ and have compared energies. As input data, the particles were given final separations of $d = 1000$ units (i.e., classical charge radii); we checked that results were not sensitive to the value of d , and followed the trajectories back through the collisions until an initial particle separation d was reached. A Hamming predictor-corrector integration routine⁸ was used. The particle energy lost during the collision was in each case in excellent agreement with the radiated energy⁹ as computed by integrating the Larmor power formula, which for motion along a straight line has the form

$$P = \frac{2}{3}\ddot{x}^2\gamma^6. \tag{6}$$

Results are summarized in Fig. 1 in which are plotted the distance of closest approach (to the or-

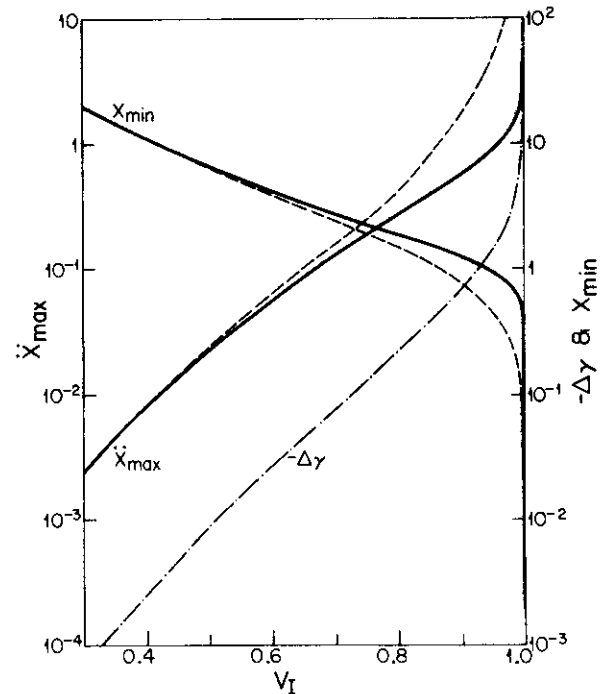


FIG. 1. Values of the turning-point position x_{min} and the maximum acceleration \ddot{x}_{max} both including radiative-reaction effects (solid lines) and omitting them (dashed lines). The dot-dashed curve gives the energy loss $-\Delta\gamma$ per particle to radiation. When radiation reaction is omitted, there is no energy loss during collision. For the curves shown here, one particle is taken to be very massive and hence fixed in position at the origin.

igin) x_{\min} , the maximum acceleration \ddot{x}_{\max} , and the particle energy loss $-\Delta\gamma$ as functions of the initial velocity V_I . For comparison, x_{\min} and \ddot{x}_{\max} are also shown for the second-order Lorentz equation, which omits radiation reaction. With radiation reaction, x_{\min} is larger than the Lorentz result [$x_{\min}^{(\text{Lorentz})} = (\gamma_I - 1)^{-1}$, $\gamma_I = (1 - V_I^2)^{-1/2}$] and \ddot{x}_{\max} is smaller ($\ddot{x}_{\max}^{(\text{Lorentz})} = x_{\min}^{(\text{Lorentz})-2}$). Furthermore, without radiation reaction, $\Delta\gamma$ is of course zero. Note that even with radiation reaction there appears to be no limit on how small x_{\min} or how large \ddot{x}_{\max} can be when $V_I \rightarrow 1$. (One would have been tempted to conclude otherwise if results had been calculated only for $V_I \leq 0.9$.)

The computed trajectories appear physically reasonable and energy is found to be conserved to high accuracy. These results support the adequacy of both our numerical techniques and the Lorentz-Dirac equation itself for particle motion in a static field.

III. SCT CALCULATIONS

The technique of integrating backward in time is successful in eliminating runaway solutions and is simple to apply to particle motion in static fields. Its application to collisions of two identical particles is considerably more complex: Use of retarded fields requires knowledge of past trajectories before they are computed. We describe here an iterative method of calculating self-consistent trajectories (SCT).

The method is similar in some respects to self-consistent field methods in calculations of atomic and molecular structures.¹⁰ We start with a trial trajectory (analogous to a trial wave function) for particle 2 from which the retarded fields are computed. A new trajectory can now be found for particle 1 by backward integration of the Lorentz-Dirac equation. The trajectory depends of course on the values of the final time, position, velocity, and acceleration (t_F , x_F , V_F , and \ddot{x}_F , respectively¹¹) with which the backward integration was started. These may be chosen to give the desired initial position and velocity and the desired turn-around time. The trajectory thus computed for particle 1 can be used for particle 2 in the next iteration. Since the trajectory at any point depends only on fields generated in the past, the iterative scheme should converge if the specified initial conditions can be attained with sufficient accuracy.

The strongest interaction between the particles occurs close to the turning points. Very slight differences in the times at turn-around change the initial values dramatically. Figure 2 shows three trajectories with slightly different turn-around times. All have the same final velocity $V_F = 0.9$,

and all were calculated with the same hyperbolic trial trajectory, namely

$$x(t) = [a^2 + (V_0 t)^2]^{1/2} + b \quad (7)$$

in which $a = 0.55$, $b = -0.1$, and $V_0 = 0.9$. The turning-point coordinates were set by changing the final t_F at which $x_F = 800$. The initial velocities are seen to vary from -0.34 to -0.98 as t_F is increased from 888.6 to 889.0. Because of this sensitivity, we found it imperative to match turning-point times precisely. In the SCT computation, matching was achieved by adjusting t_F until $V(0) \simeq 0$. With such matching performed at each step, V_F was then adjusted to give the desired initial velocity V_I . After both $V(0)$ and V_I were correctly set, the x axis was shifted to equalize the distances of closest approach of the two particles. Then the iteration was complete, and the computed trajectory was used to determine retarded fields on the next iteration. The procedure was continued until trajectories computed on successive iterations became equal to within small limits.

Several factors complicate the iteration scheme. In Fig. 2 the path of the turning point ($x_{\text{TP}}, t_{\text{TP}}$) is shown as t_F is varied and V_F held fixed at 0.90 (dotted curve). It is obvious that t_{TP} is not a linear function to t_F . In fact, at high velocities there may

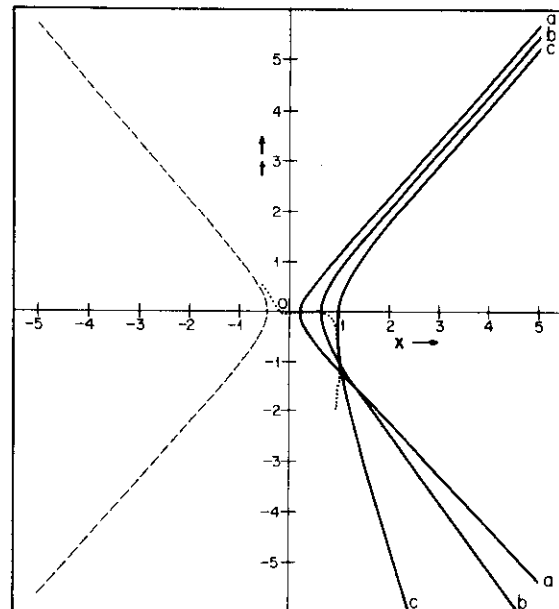


FIG. 2. Trajectories of particle 1 with slightly different final times t_F : curve *a* has $t_F = 889.0$, curve *b* has $t_F = 888.8$, and curve *c* has $t_F = 888.6$. In each case the trajectory of particle 2 (dashed curve) is the same, namely the trial hyperbolic trajectory of Eq. (7). The dotted curve gives the variation of turning-point position as t_F is varied.

be one, two, or three values of t_F which give the desired match $t_{TP} = 0$, as can be seen in Fig. 3 where turning-point paths are plotted for $V_F = 0.89, 0.90, \text{ and } 0.91$. The trajectories associated with the different turning-point positions may have greatly different initial velocities, V_I . For turning points occurring at $x_{TP} < 0$, V_I is usually too high, namely $V_I > 0.9999$. However, for final velocities V_F slightly less than some limit V_{lim} (≈ 0.9 in Fig. 3), the turning-point path crosses the x axis at two larger values of x_{TP} . Consequently, for each V_F slightly less than V_{lim} , there are two possible trajectories with different V_I but both with $t_{TP} = 0$. A small change in V_F can cause roughly an order of magnitude larger change in V_I . At higher velocities, trajectories are even more sensitive to V_F and t_{TP} . However, these are merely computational complications and should not affect the final trajectory; for a given trajectory of particle 2, there always seems to be a *unique* choice of t_F and V_F which give $t_{TP} = 0$ and the desired value of V_I for particle 1.

In a typical computation, ten iterations are per-

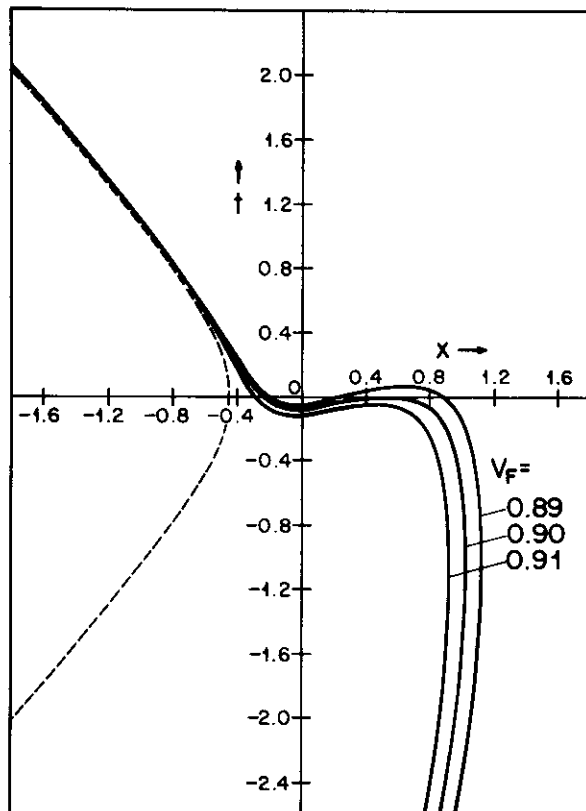


FIG. 3. Turning-point paths for particle 1 for three different trial velocities V_F . The trajectory of particle 2 is given by the dashed curve to the left.

formed with increasingly stringent accuracy requirements. Within each iteration about 20 trajectories must be computed with different values of t_F and V_F in order to reach a V_I with the desired value and $t_{TP} \approx 0$. In each iteration all points of the last trajectory calculated during the predictor-corrector integration are stored for use in calculating retarded fields on the subsequent iteration. On the last two iterations, the integration error was held to $\leq 5 \times 10^{-9}$, t_F was adjusted to within 4×10^{-5} of the values required to give $t_{TP} = 0$, and V_I was set to within 4×10^{-6} of the desired value. The maximum differences in the last two iterations calculated were generally about 5×10^{-4} in $x(t)$, 8×10^{-7} in $\dot{x}(t)$, and 5×10^{-7} in $\ddot{x}(t)$. All calculations were made in "double precision" (about 15 digits) on an IBM 360-65 computer.

On the first iteration the trial trajectory for particle 2 was the hyperbola of Eq. (7) with parameters a and b adjusted by trial and error. Final and initial separations of between 10^3 and 3×10^3 were used, together with final accelerations between $\gamma^{-3}E$ and $\gamma^{-3}E(1 + 2\dot{x}E)$, where E is the electric field

$$E = (x + x_R)^{-2}(1 - V_R)/(1 + V_R), \quad (8)$$

with x_R and $V_R \equiv \dot{x}(t_R)$ the position and velocity, respectively, at the retarded time t_R . It was verified that the final trajectory did not depend significantly on either the final separation, the trial trajectory, or the final acceleration.

IV. RESULTS

All the trajectories calculated here seem physically reasonable. The colliding particles always lost a small fraction of their kinetic energy during the collision to radiation, and compared with computations without radiation reaction, the maximum accelerations were smaller and the minimum distances of closest approach were larger (see Fig. 4).

We were at first surprised that the energy loss was much less than the radiated energy as calculated by the Larmor power formula [Eq. (6)]. We should not have been. The radiation fields of the two particles of equal mass largely interfere and result in a much smaller energy loss than twice the radiative loss of a single particle. The basic mode is quadrupole radiation rather than dipole. Since different directions in space generally receive radiation from *different relative* positions along the trajectories of the particles, it did not appear possible to derive a simple expression valid for all collision velocities for the total power radiated.

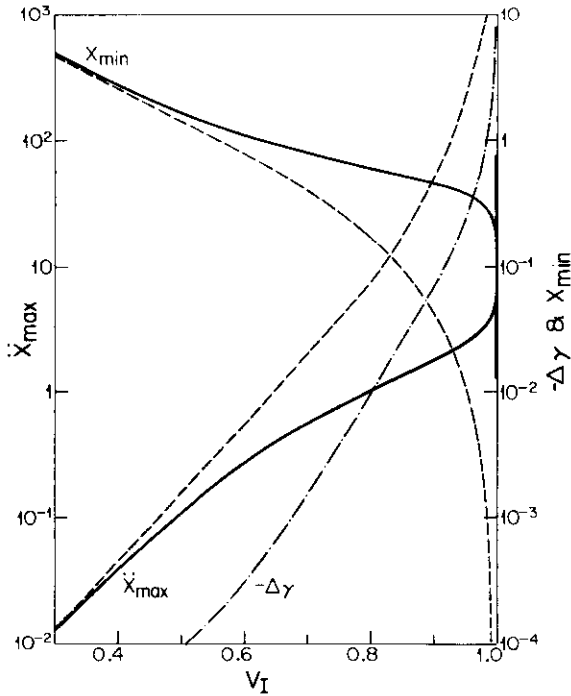


FIG. 4. Same as for Fig. 1, but now for two particles of equal mass. (In this case, when radiation reaction is omitted, the particles *gain* energy during collision.)

If velocities are sufficiently low that retardation effects between the particles can be ignored, then the power formula for quadrupole radiation can be applied.¹² As far as we are aware, the results presented here are the first calculations of radiation from like particles colliding at high velocities.

SCT runs were made for incident velocities to $V_I = 0.99$. As seen in Fig. 4, the results for $V_I \leq 0.95$ appear to extrapolate to a nonzero distance of closest approach and a finite acceleration and energy loss in the limit $V_I \rightarrow 1$. The results for $V_I = 0.98$ and 0.99 demonstrate the danger of such extrapolations. As the incident energy is increased, there appears to be no limit to how close the particles come, how much energy they lose, or how large the maximum acceleration becomes. In Fig. 5, trajectories for $V_I = 0.8$ are compared with and without radiation reaction. With radiation reaction, the particles are seen to turn around at slightly later times with lower acceleration and at larger separations. Also the velocities after collision are slower with radiation reaction. The maximum acceleration is reached after t_{TP} even though the change in velocity before t_{TP} is greater than that after. In Fig. 4 comparison of results with and

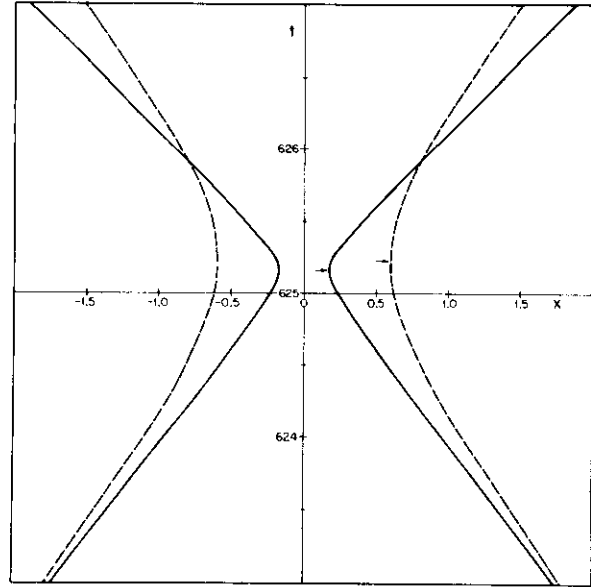


FIG. 5. A comparison of self-consistent trajectories with (dashed line) and without (solid line) radiation reaction for initial velocities $V_I = 0.8$. Arrows indicate the turning points. Particles were started for this plot at $t = 0$, with $x_I = 500$.

without radiation reaction are made as a function of V_I . The change in kinetic energy per particle $\Delta\gamma$ is not shown on the plot of $\log(-\Delta\gamma)$ for the Lorentz equation since without radiation reaction $\Delta\gamma > 0$.¹

We have thus demonstrated that for head-on collisions of two like particles, the classical Lorentz-Dirac equation can be solved to yield physical solutions for incident velocities at least up to $V_I = 0.99$. At the highest velocities for which computations were made, the particles come to within a classical charge radius of each other ($2x_{min} = 0.515$ for $V_I = 0.99$). Although a rather complex SCT scheme was required to obtain the solutions, the results themselves hold no real surprises: The trajectories appear entirely reasonable. The present calculations, we feel, lend support to the validity and applicability of the Lorentz-Dirac equation as a classical description of collisions of like-charged point particles at relativistic velocities.

In the following paper¹³ we report on our calculations of head-on collisions of oppositely charged point particles. There, difficulties with the Lorentz-Dirac solutions do arise.

*Work supported by the National Research Council of Canada.

¹J. Huschilt, W. E. Baylis, D. Leiter, and G. Szamosi, *Phys. Rev. D* **7**, 2844 (1973).

²"Nonlocal" is a more precise description of the character of the Lorentz-Dirac equation; see F. Rohrlich, in *Physical Reality and Mathematical Description*, edited by C. P. Enz and J. Mehra (Reidel, Boston, Mass., 1974), p. 387. However, the effects of non-locality are often viewed as pathological; see for example Ref. 4.

³F. Rohrlich, *Classical Charged Particles* (Addison-Wesley, Reading, Mass., 1965), especially Chap. 6. A simple derivation of the Lorentz-Dirac equation, requiring only retarded fields, has been given by A. O. Barut, *Phys. Rev. D* **10**, 3335 (1974).

⁴Tse Chin Mo and C. H. Papas, *Phys. Rev. D* **4**, 3566 (1971).

⁵J. Huschilt and W. E. Baylis, *Phys. Rev. D* **9**, 2479 (1974).

⁶G. N. Plass, *Rev. Mod. Phys.* **33**, 37 (1961).

⁷For example, J. D. Jackson, *Classical Electrodynamics* (Wiley, New York, 1962), Chap. 14 and Ref. 3, Chap. 5.

⁸A. Ralston and H. S. Wilf, *Mathematical Methods for*

Digital Computers (Wiley, New York, 1960), Vol. I, Chap. 8.

⁹Initially, before the particles begin to interact, the entire field energy is that of the bound (i.e., Lorentz-transformed Coulomb) fields, which is identical to the initial unrenormalized particle energy. Finally, once the particles have completed their interaction and have vanishing acceleration (required for a physical solution), the total field energy consists of that of the bound fields plus the radiated (free-field) energy. Consequently conservation of energy requires that the change in particle energy balance the energy radiated.

¹⁰For example, J. C. Slater, *Quantum Theory of Atomic Structure* (McGraw-Hill, New York, 1960), Vol. I, Chap. 9.

¹¹To ensure a physical solution, \ddot{x}_F is always chosen to be small, namely roughly equal to the value prescribed by the second-order Lorentz equation. In fact, the SCT trajectory is relatively insensitive to the value of \ddot{x}_F used (see below).

¹²L. Landau and E. Lifshitz, *The Classical Theory of Fields* (Addison-Wesley, Reading, Mass., 1962), Chap. 9.

¹³W. E. Baylis and J. Huschilt, following paper, *Phys. Rev. D* **13**, 3262 (1976).